

1 **cGAS Expression is Enhanced in Systemic Sclerosis Associated Interstitial Lung**
2 **Disease and Stimulates Inflammatory Myofibroblast Activation**

3 Sheeline Yu¹, Buqu Hu¹, Ying Sun¹, Xue Yan Peng¹, Chris J. Lee¹, Samuel Woo¹, John
4 McGovern¹, Jana Zielonka¹, Tina Saber¹, Alexander Ghincea¹, Shifa Gandhi¹, Anjali Walia¹,
5 Taylor Pivarnik¹, Genta Ishikawa¹, Shuai, Shao¹, Huanxing Sun¹, Baran Ilayda Gunes², Sophia
6 Kujawski², Stephanie Perez², William Odell², Monique Hinchcliff², John Varga³, Carol Feghali-
7 Bostwick⁴, Maor Sauler¹, Jose L. Gomez¹, *Changwan Ryu¹, *Erica L. Herzog^{1,5}

8 ¹Yale School of Medicine, Section of Pulmonary, Critical Care, and Sleep Medicine

9 ²Yale School of Medicine, Department of Internal Medicine, Section of Rheumatology, Allergy,
10 and Immunology

11 ³University of Michigan, Department of Internal Medicine, Division of Rheumatology

12 ⁴Medical University of South Carolina, Department of Medicine

13 ⁵Yale School of Medicine, Department of Pathology

14 *Equally contributed to this work
15

16 **Corresponding author**

17 Erica L. Herzog

18 Email: erica.herzog@yale.edu
19

20 **Contributions**

21 SY conducted the investigation, interpreted data, and wrote and edited the manuscript. BH, YS,
22 XYP, CJL, SW, JM, JZ, TS, AG, SG, AW, TP, SS, HS, MS, and JLG performed the investigation
23 and analyzed data. BIG, SK, SP, WO, and MH recruited subjects, performed the investigation,
24 and analyzed data. JV provided conceptualization, resources, supervision, and funding
25 acquisition. CFB provided conceptualization and resources. CR and ELH provided
26 conceptualization, resources, supervision, project administration, funding acquisition, and wrote
27 and edited the manuscript. All authors participated in manuscript preparation and provided final
28 approval of the submitted work.
29

30 **Funding**

31 JZ was supported by T32HL007778. AG was supported by T32HL007778. GI was supported by
32 a Scholar Award from the Pulmonary Fibrosis Foundation, Wit Family Distinguished Scholar in
33 Inflammation Science, and Yale Physician Scientist Development Award. MH was supported by
34 R01 AR073270. JG was supported by R01HL153604 and R03 HL154275. CR was supported by
35 K08HL151970-01 and Boehringer-Ingelheim Discovery Award. ELH was supported by
36 5R01HL163984-02 and 5R01HL152677-04. The content is solely the responsibility of the
37 authors and does not necessarily represent the official views of the National Institutes of Health
38 or other funding sources.
39

40 **Word Count:**

41 3609 words
42

43 **TAKE HOME MESSAGE**

44 Using various translational models of SSc-ILD, we found that activation of the innate immune
45 receptor cGAS contributes to inflammatory myofibroblast phenotypes that are attenuated by
46 inhibiting this receptor.

47

48 **ABSTRACT**

49 **Objective:** The lungs of patients with Systemic Sclerosis Associated Interstitial Lung Disease
50 (SSc-ILD) contain inflammatory myofibroblasts arising in association with fibrotic stimuli and
51 perturbed innate immunity. The innate immune DNA binding receptor Cyclic GMP-AMP
52 synthase (cGAS) is implicated in inflammation and fibrosis, but its involvement in SSc-ILD
53 remains unknown. We examined cGAS expression, activity, and therapeutic potential in SSc-
54 ILD using cultured fibroblasts, precision cut lung slices (PCLS), and a well-accepted animal
55 model.

56 **Methods:** Expression and localization of cGAS, cytokines, and type 1 interferons were
57 evaluated in SSc-ILD lung tissues, bronchoalveolar lavage (BAL), and isolated lung fibroblasts.
58 CGAS activation was assessed in a publicly available SSc-ILD single cell RNA sequencing
59 dataset. Production of cytokines, type 1 interferons, and α SMA elicited by TGF β 1 or local
60 substrate stiffness were measured in normal human lung fibroblasts (NHLFs) via qRT-PCR,
61 ELISA, and immunofluorescence. Small molecule cGAS inhibition was tested in cultured
62 fibroblasts, human PCLS, and the bleomycin pulmonary fibrosis model.

63 **Results:** SSc-ILD lung tissue and BAL are enriched for cGAS, cytokines, and type 1 interferons.
64 The cGAS pathway shows constitutive activation in SSc-ILD fibroblasts and is inducible in
65 NHLFs by TGF β 1 or mechanical stimuli. In these settings, and in human PCLS, cGAS
66 expression is paralleled by the production of cytokines, type 1 interferons, and α SMA that are
67 mitigated by a small molecule cGAS inhibitor. These findings are recapitulated in the bleomycin
68 mouse model.

69 **Conclusion:** cGAS signaling contributes to pathogenic inflammatory myofibroblast phenotypes
70 in SSc-ILD. Inhibiting cGAS or its downstream effectors represents a novel therapeutic
71 approach.

72 **Word Count:** 250 words

73

74 **Key Words:** (1) Systemic Sclerosis; (2) Interstitial Lung Disease; (3) cGAS; (4) inflammatory
75 myofibroblast

76

77 INTRODUCTION

78 Systemic Sclerosis (SSc) is an autoimmune condition characterized by progressive
79 fibrosis of the skin and visceral organs [1]. Patients with SSc frequently develop interstitial lung
80 disease (SSc-ILD), a pulmonary condition characterized by inflammatory cell infiltration and
81 fibrotic remodeling [2]. SSc-ILD underlies the considerable morbidity and mortality in patients
82 with SSc [3], and current consensus treatment guidelines recommend immunosuppressive
83 agents and anti-fibrotic drugs that are not universally effective and impose significant burden in
84 terms of side effects and cost [4-6]. Thus, understanding the mechanisms contributing to both
85 inflammation and fibrosis is imperative for the development of effective treatments to improve
86 patient care.

87 The lungs of patients with SSc-ILD exhibit varying degrees of immune activation and
88 extracellular matrix (ECM) accumulation [2]. Additionally, the lungs contain heterogeneous
89 fibroblast populations that produce inflammatory mediators, secrete collagens and other ECM
90 molecules, and express myofibroblast markers such as alpha smooth muscle actin (α SMA) [7-
91 9]. These properties are inducible in normal human lung fibroblasts (NHLFs) by fibrotic stimuli,
92 including transforming growth factor beta 1 (TGF β 1) [10] and interactions with stiffened tissue
93 substrates [11]. The presence of inflammatory myofibroblasts in SSc-ILD may account for
94 heterogeneous treatment responses as currently used first-line treatments are designed to
95 either suppress the inflammatory function of immune cells or the fibrogenic function of
96 fibroblasts. Missing from our therapeutic strategies are agents that can simultaneously mitigate
97 inflammation and fibrogenesis in a single population of fibroblast effector cells. In view of these
98 limitations, the identification of druggable pathways that simultaneously contribute to
99 inflammatory responses and fibrotic functions in fibroblasts remains a critical unmet need.

100 Innate immune drivers of fibroblast activation have emerged as important pathogenic
101 pathways in SSc-ILD. Of particular interest are nucleic acid receptors that recognize and

102 respond to DNA and RNA derived from invading pathogens and injured cells. We and others
103 have demonstrated vital roles for Toll-like receptor 9 in fibroblast activation and disease
104 progression in SSc-ILD and associated conditions [11-13]. In contrast, the pathogenic
105 contribution of alternate nucleic acid receptors, such as cyclic guanosine monophosphate-
106 adenosine monophosphate synthase (cGAS), remains less well understood. The broadly
107 expressed intracellular receptor cGAS is a nucleotidyltransferase that, upon binding to cytosolic
108 DNA derived from invading pathogens or endogenous sources (nuclei, mitochondria), catalyzes
109 the production of 2,3-cGAMP [14]. This substrate then activates the cytosolic kinase stimulator
110 of interferon genes (STING) to initiate production of interferon regulatory factor-3 (IRF3) and
111 nuclear factor- κ B (NF κ B) dependent proinflammatory cytokines, chemokines, and type I
112 interferons in immune cells [15]. Reflecting the emerging importance of cGAS in disease
113 development, numerous approaches to cGAS-STING modulation exist in the therapeutic
114 pipeline for conditions of chronic inflammation and autoimmunity [15, 16]. Intriguingly, the
115 cGAS-STING pathway has also been implicated as a fibroblast activator in diverse conditions
116 such as cancer [17], aging [18], pulmonary fibrosis [19], and SSc [20]; and endogenous cGAS
117 ligands such as DNA from mitochondria (mtDNA) and nuclear sources are elevated in patients
118 with SSc [12, 13, 20]. However, the mechanistic and therapeutic potential of cGAS in SSc-ILD is
119 currently unknown.

120 On the basis of this biology, we surmised that engagement of cGAS drives inflammatory
121 myofibroblast accumulation in SSc-ILD. To test this hypothesis, we evaluated the expression
122 and function of cGAS in patient samples, *ex vivo* modeling systems, and in a well-accepted
123 mouse model. Our results show that expression of cGAS and its associated inflammatory
124 mediators is increased in lung tissue and bronchoalveolar lavage (BAL) fluid from SSc-ILD
125 patients, where it is constitutively expressed and activated in SSc-ILD fibroblasts, and inducible
126 in NHLFs following stimulation with either TGF β 1 or mechanical stimuli. In these settings, and in

127 human precision cut lung slices (PCLS), cGAS expression is paralleled by production of
128 inflammatory mediators and α SMA expression that are mitigated by a small molecule cGAS
129 inhibitor. Similar anti-fibrotic effects of cGAS inhibition are seen in an experimental model of
130 mouse lung fibrosis. Altogether, our compelling results implicate cGAS in inflammatory fibroblast
131 activation and fibrosis underlying SSc-ILD pathogenesis, putting forth cGAS inhibition as a novel
132 therapeutic in this disease.

133

134 **MATERIALS AND METHODS**

135 Detailed methods are provided in the online supplement.

136

137 **Human Subjects**

138 De-identified lung tissues and primary lung fibroblasts that had been previously obtained at the
139 University of Pittsburgh (IRB 970946), and de-identified BAL fluid specimens that had been
140 previously collected from healthy donors and patients with SSc using informed consent on
141 protocols approved by Institutional Review Board at the Yale School of Medicine (HIC
142 2000024862), were used in this study.

143 **Single Cell RNA Sequencing (scRNA seq) Analysis**

144 Analyses of scRNA seq data (GSE128169) were performed with Seurat version 5.0.318 as
145 described in the online supplement. To identify cell types expressing genes associated with
146 cGAS, the AddModuleScore, a Seurat function that calculates the gene expression level of a
147 cluster of genes on a single cell level and then subtracts the aggregated expression of a
148 randomly assigned control set, was used.

149 **Fibroblast Cultures**

150 Fibroblasts harvested from the lungs of patients with SSc-ILD were cultured in the absence or
151 presence of the small molecule cGAS inhibitor G140 (10 μ M, Invivogen). NHLFs were cultured
152 in the absence or presence of recombinant human TGF β 1 (5 ng/ml) and CpG ODN2006 (50
153 μ mol) and in the absence or presence of G140. In parallel, NHLFs were cultured on collagen-
154 coated hydrogels (Matrigen) of 1 kPA and 25 kPA stiffness in the absence or presence of G140.

155 **Human PCLS**

156 PCLS from normal human donors (Institute for In Vitro Sciences) were incubated in culture
157 media supplemented with or without an inflammatory fibrotic cocktail (IFC) comprised of the
158 following: TGF β 1 (5 ng/ml), platelet-derived growth factor-AB (PDGF-AB, 5 μ M), tumor necrosis
159 factor alpha (TNF- α , 10 ng/ml), lysophosphatidic acid (LPA, 5 μ M), and CpG ODN2006 (50
160 μ mol); PCLS subjected to this cocktail were then treated in the absence or presence of G140
161 (10 nM).

162 **Mouse Experiments**

163 Animal procedures were approved by the Yale Institutional Animal Care and Use Committee.
164 C57Bl/6 mice received a single dose of inhaled bleomycin (0.8 units/kg) or normal saline.
165 Vehicle control or G140 (30 mg/kg) was administered via intraperitoneal injection on days 3, 7,
166 and 10 post-bleomycin. Mice were euthanized on day 14 and biospecimens were collected for
167 analysis.

168 **RNA Isolation and qRT-PCR**

169 Total cellular RNA was isolated and reverse transcribed for *GAPDH*, *ACTA2*, and *CGAS* from
170 biospecimens as described in the online supplement.

171 **Cell Lysis**

172 Cells were washed and lysed in a solution containing Pierce RIPA buffer and a Halt™ Protease
173 Inhibitor Cocktail (ThermoFisher).

174 **Quantification of Cytokines**

175 Multiplex quantification of interleukin-6 (IL-6), interleukin 1-beta (IL-1β), tumor necrosis factor
176 alpha (TNF-α), monocyte chemoattractant protein-1 (MCP-1), interferon-gamma inducible
177 protein-10 (IP-10), interferon alpha (IFN-α), and interferon beta (IFN-β) using the U-PLEX
178 Cytokine Panel Human Kit or U-Plex Cytokine Panel Mouse Kit (Mesoscale Discovery).

179 **ELISA**

180 Cell lysates were assayed for αSMA (Abcam) or cGAS (Cell Signaling Technology) via
181 commercially available ELISA as described in the online supplement.

182 **MTT Assay**

183 Cell viability was determined using MTT assays (Thermofisher) as described in the online
184 supplement.

185 **cGAS Immunohistochemistry (IHC)**

186 Formalin fixed, paraffin embedded slides of human lung tissue from healthy or SSc-ILD donors
187 (n=4/each) were stained with a human cGAS antibody (1:100, Invitrogen) as described in the
188 online supplement. cGAS quantification was performed by manually counting total nuclei and
189 nuclei from cGAS-expressing cells; results were reported as the percentage of positive cGAS
190 cells per high-power field.

191 **Immunofluorescence (IF)**

192 IF detection of α SMA and cGAS in fibroblasts were performed with mouse anti- α SMA (1:250,
193 Abcam) and rabbit monoclonal cGAS (1:100, Invitrogen) antibodies as described in the online
194 supplement.

195 **Lung Histology**

196 Formalin fixed, paraffin embedded lung sections from PCLS or mouse lungs were stained with
197 Masson's trichrome [21]. Collagen was quantified with ImageJ software as described in the
198 online supplement. Soluble collagen was quantified using the Sircol Collagen Assay kit
199 (Biocolor) [22].

200 **Bulk RNA Sequencing**

201 RNA isolated from PCLS was sequenced on the Illumina NovaSeq platform as described in the
202 online supplement. Differential gene expression was identified with the DESeq2 package on R
203 statistical software (version 4.3.2). Heatmaps were generated in R with the gplots package.
204 Pathway enrichment analysis was conducted via MetaCore; a false discovery rate (FDR) < 0.10
205 was considered significant.

206 **Statistical Analysis**

207 Data distribution was assessed using Shapiro-Wilk test, and categorical data was analyzed with
208 Fisher's exact test using GraphPad Prism 9.4.1. Multiple hypothesis testing was conducted with
209 one-way ANOVA with Bonferroni correction with GraphPad Prism. Pairwise comparisons were
210 conducted with an unpaired t-test or Mann Whitney test based on data distribution with
211 GraphPad Prism. p-values < 0.05 were considered significant.

212

213 **RESULTS**

214 **Expression of cGAS and its associated soluble mediators are enriched in the lungs of**
215 **patients with SSc-ILD**

216 To assess a potential relationship between cGAS and SSc-ILD, IHC was performed on lung
217 tissues obtained from control (unsuitable organ donors) or SSc-ILD patients undergoing
218 orthotopic lung transplantation. In contrast to the low level of cGAS detection observed in
219 control samples, SSc-ILD lung tissues displayed abundant cGAS expression in cells exhibiting
220 the morphology of immune populations, epithelium, and fibroblasts (Figures 1A,B). cGAS-
221 associated soluble mediators were then measured in BAL specimens from control and SSc
222 donors shown in Table 1. Compared to healthy controls, SSc-ILD BAL showed high
223 concentrations of cytokines (IL-6, IL-1 β , TNF- α , Figures 1C-E), chemokines (MCP-1, IP-10,
224 Figures 1F,G), and type 1 interferons (IFN- α , IFN- β , Figures 1H,I) all of which are known to be
225 downstream of cGAS activation. These data show that the lungs of patients with SSc-ILD show
226 strong expression of cGAS and its associated soluble mediators.

227 **Enhanced expression and activation of cGAS in SSc-ILD fibroblasts**

228 Having identified enhanced cGAS expression in SSc-ILD lung tissues, we then investigated this
229 biology in disease-relevant cell types. We began by analyzing a publicly available scRNA seq
230 dataset (GSE128169) generated from end-stage SSc-ILD lung explants. Consistent with our
231 IHC findings above, multiple cell populations showed transcriptional evidence of cGAS
232 activation (Figures S1 and 2A). When this analysis was limited to stromal cells, fibroblasts
233 exhibited high expression of cGAS pathway transcripts (Figure 2B). These *in silico* studies were
234 confirmed *in vitro* with primary lung fibroblasts, where evaluation of cGAS expression via qRT-
235 PCR and ELISA showed increased expression at the mRNA and protein levels (Figures 2C,D).
236 Moreover, IF analysis revealed that the baseline nuclear cGAS localization seen in NHLFs was
237 accompanied by the detection of cytoplasmic aggregates in SSc-ILD fibroblasts, indicating that
238 these cells may exist in a state of heightened cGAS activation (Figures S2 and 2E). Importantly,

239 this phenotype was accompanied by increased production of cGAS-associated inflammatory
240 mediators (IL-6, IL-1 β , TNF- α , MCP-1, IP-10, IFN- α , IFN- β) along with elevated mRNA and
241 protein levels of the myofibroblast marker α SMA (Figures 3A-I). These results implicate cGAS
242 as a driver of inflammatory myofibroblast activation in SSc-ILD.

243 **A small molecule cGAS inhibitor mitigates inflammatory mediator production and fibrotic** 244 **activation of SSc-ILD fibroblasts**

245 To link cGAS more firmly with inflammatory myofibroblast activation in SSc-ILD, we performed
246 loss of function studies using the cGAS inhibitor G140. This commercially available, highly
247 specific small molecule inhibitor blocks DNA entry into human cGAS catalytic pocket to impede
248 enzymatic activation [23]. In our study, treatment of SSc-ILD fibroblasts with G140 reduced
249 cytoplasmic cGAS aggregates (Figure 4A), suggesting successful inhibition. This observation
250 was paralleled by decreased production of inflammatory mediators (IL-6, IL-1 β , TNF- α , MCP-1,
251 IP-10, IFN- α , and IFN- β , Figures 4B-H). G140 treatment also reduced α SMA mRNA measured
252 by qRT-PCR (Figure 4I) and protein measured by IF and ELISA (Figures 4A,J). Importantly,
253 these findings were not due to alterations in cellular viability as the results of an MTT assay
254 were similar between untreated and treated cells (Figure 4K). These studies show that cGAS
255 inhibition reduces production of cytokines, chemokines, type 1 interferons, and α SMA
256 expression in SSc-ILD fibroblasts, providing proof of concept evidence for targeting cGAS in this
257 disease.

258 **Small molecule cGAS inhibition suppresses TGF β 1 and CpG induced fibroblast** 259 **activation**

260 Studies of diseased lung fibroblasts are useful for the development of mechanistic-based SSc-
261 ILD therapies. However, while providing evidence of target engagement, they are limited by the
262 end-stage nature of the disease. Because the therapeutic goal is to prevent clinical progression,

263 studies aimed at preventing cellular activation have the potential to halt or even reverse
264 disease. Reasoning that fibroblasts adopt their ultimate phenotype in response to
265 microenvironmental cues, we developed a model of cGAS activation in which NHLFs were co-
266 stimulated with TGF β 1 and CpG ODN2006 to simulate the endogenous cGAS ligand mtDNA
267 (Figures S3A,B). Following co-stimulation, NHLFs phenocopied many aspects of SSc-ILD
268 fibroblasts, including increased expression and cytoplasmic aggregation of cGAS (Figures S4A-
269 C), production of inflammatory mediators (IL-6, IL-1 β , TNF- α , MCP-1, IP-10, IFN- α , IFN- β ,
270 Figures S4D-J), and α SMA mRNA and protein (Figures S4K,L). These changes were cGAS-
271 dependent as treatment with G140 diminished cytoplasmic cGAS aggregation (Figure 5A) and
272 suppressed production of all inflammatory mediators except for IL-6 (Figures 5B-H). Production
273 of α SMA mRNA and protein were also reduced (Figures 5I,J). Lastly, a MTT assay revealed
274 these findings to be unrelated to changes in cell viability (Figure 5K). Taken together, these data
275 provide evidence of cGAS antagonism as a novel strategy of mitigating the fibroblast activation
276 that arises in response to TGF β 1 and endogenous cGAS ligands.

277 **A small molecule cGAS inhibitor opposes stiffness-induced fibroblast activation**

278 Cells encounter and respond to physical properties, such as stiffness, in their microenvironment.
279 While cGAS has been previously linked to fibrotic mechanosensing [18], its involvement in SSc-
280 ILD and therapeutic targeting in lung fibroblasts remains underexplored. Thus, we investigated
281 this area using tunable hydrogels constructed to simulate the stiffness of normal (1 kPA) or SSc-
282 ILD (25 kPA) lung [24]. Compared to cells cultured under physiologic conditions, NHLFs grown
283 on 25 kPA gels developed increased cGAS mRNA transcription and protein levels (Figures
284 S5A,B), secretion of IL-1 β , MCP-1, IP-10, IFN- α , and IFN- β , but not IL-6 or TNF- α (Figures
285 S5C-I) as well as induction of α SMA mRNA and protein expression (Figures S5J,K). Treatment
286 with G140 reduced IL-1 β , IP-10, IFN- α , and IFN- β , but not MCP-1 (Figures 6A-E), and
287 attenuated α SMA mRNA and protein (Figures 6F,G) without affecting cellular viability (Figure

288 6H). Overall, these data frame cGAS as a druggable driver of mechanosensitive fibroblast
289 responses that are pathogenic in SSc-ILD.

290 **A small molecule cGAS inhibitor suppresses inflammatory mediator production and**
291 **fibrotic endpoints in human PCLS**

292 Studies of isolated lung fibroblasts provide direct evidence of cell autonomous responses in
293 these fibrotic cells. However, they are limited by the lack of information regarding the complex
294 multicellularity of the adult lung, which can activate fibroblasts via non-cell autonomous
295 processes. To overcome these issues, we extended our studies to include PCLS, an advanced
296 *in vitro* modeling system that allows previously impossible tissue level insights into human lung
297 injury, repair, and remodeling. This technology improves upon standard primary monoculture
298 methods by replicating the complex 3D topography and multicellularity of the lung [25]. Our
299 preliminary studies used a model of normal PCLS cultured in media containing an inflammatory
300 fibrotic cocktail (IFC) of TGF β , PDGF-AB, TNF- α , and LPA, and supplemented with the mtDNA
301 surrogate CpG ODN2006. As compared to naïve PCLS, those cultured in this IFC displayed
302 enhanced collagen content (Figures S6A-B), cGAS transcripts (Figure S6C), protein levels of IL-
303 6, IL-1 β , TNF- α , MCP-1, IP-10, and IFN- α , but not IFN- β (Figures S6D-J). α SMA transcripts
304 were also increased (Figure S5K). Treatment with the cGAS inhibitor G140 reduced all these
305 endpoints (Figures 7A-I). Lastly, to identify parallel transcriptional changes that occur in the
306 absence or presence of G140, we conducted exploratory bulk RNA sequencing and identified
307 126 differentially expressed genes (Figure 7J). Unbiased pathway enrichment analysis revealed
308 a multitude of transcriptional changes involving inflammatory and immune function with the most
309 highly altered pathways being related to cytoskeletal remodeling, IL-17, cell adhesion, antigen
310 presentation, NF- κ B activation, interferon beta signaling, and mesenchymal cell activation
311 (Figure 7K). The finding that cGAS inhibition suppresses production of cytokines, chemokines,
312 type 1 interferons, α SMA expression, and collagen production during human lung fibrogenesis

313 suggests that targeting cGAS and/or its associated pathways holds therapeutic potential in SSc-
314 ILD.

315 **A small molecule cGAS inhibitor mitigates bleomycin-induced pulmonary fibrosis**

316 Finally, having demonstrated the benefit of a cGAS inhibitor in orthogonal *ex vivo* modeling
317 experiments, we sought to determine its efficacy *in vivo*. For this purpose, we used the
318 bleomycin model of fibrosis in mice, which is the most widely accepted SSc-ILD animal model
319 [2]. Mice were subjected to orotracheal instillation of either normal saline or bleomycin in
320 presence of vehicle or G140. As shown in Figures S7A-C, bleomycin challenged mice exhibited
321 greater lung collagen accumulation than those that received normal saline or G140 alone.
322 Evaluation of BAL fluid revealed elevations of IL-6, IL-1 β , TNF- α , MCP-1, IP-10, IFN- α , and IFN-
323 β (Figures S7D-J). When bleomycin-challenged mice were treated with G140, we observed
324 marked reductions in lung collagen content (Figures 8A-C) and BAL concentrations of IL-6,
325 TNF- α , IP-10, IFN- α , and IFN- β , but not IL-1 β and MCP-1 (Figures 8D-J). When viewed in
326 combination, our results identify cGAS as a modulator of inflammatory fibroblast activation in
327 mammalian lung fibrosis and supports the clinical development of cGAS inhibitors for treatment
328 of SSc-ILD.

329

330 **DISCUSSION**

331 Innate immunity and inflammatory myofibroblast activation are increasingly linked to
332 SSc-ILD; however, their mechanistic and therapeutic implications are not well understood [26].
333 Here we identified the cytosolic DNA sensor cGAS as a mechanistic driver of and therapeutic
334 target in SSc-ILD. Our results revealed that expression of cGAS and its downstream mediators
335 are enhanced in SSc-ILD lung tissues, BAL fluid, and lesional fibroblasts. These findings are
336 recapitulated in SSc-ILD modeling systems, including NHLFs exposed to biochemical and

337 biophysical fibrotic stimuli, human PCLS exposed to fibrogenic mediators, and the well accepted
338 bleomycin mouse model. A small molecule cGAS inhibitor exerted an anti-inflammatory and
339 antifibrotic effects in all these settings. Targeting aberrant cGAS activation holds promise as an
340 innovative strategy in SSc-ILD, as well for myriad other inflammatory fibrosing conditions
341 characterized by autoimmunity [27], neurodegeneration [28], cancer [17], and aging [18].

342 Upon its 2013 discovery, cGAS was described as a nucleotidyltransferase that
343 recognizes pathogen-derived DNA and activates type 1 interferon production in a STING-
344 dependent, IRF3 dependent manner [14]. Since this time, cGAS has been shown to be
345 activated by endogenous DNA, including that derived from nuclei and mitochondria [10]. cGAS
346 can recognize self-ligands that leak into the cytoplasm following DNA damage responses or
347 mitochondrial stress, or that which have been internalized as damage associated molecular
348 patterns (DAMPs) present in the extracellular milieu. Our prior work implicated mtDNA as a
349 putative cGAS activator [10] and the present study advances this notion as we were able to
350 induce fibroblast activation and cGAS signaling with the administration of exogenous CpG, a
351 surrogate for cell-free mtDNA. Further work characterizing the nature of mtDNA and its
352 interactions with cGAS has the potential to elucidate intervenable innate immune mechanisms
353 of inflammatory fibroblast activation in SSc-ILD.

354 The results reported herein are predicated on the ability of cGAS to activate STING and
355 induce NFkB and IRF3 signaling [14]. In our work, cGAS inhibition suggested context
356 dependent aspects of the various modeling systems. For example, while SSc-ILD BAL and
357 fibroblasts are enriched for NFkB-dependent and IRF3-dependent cytokines and type 1
358 interferons, we have not characterized the contribution of STING and its associated transcription
359 factors in our work. The expression of NFkB and IRF3 dependent inflammatory mediators
360 supports pleiotropic effect, and the effect on α SMA expression likely reflects the recently
361 described role of cGAS-STING in canonical TGF β 1 activation and YAP/TAZ mediated

362 mechanosensing. It is equally possible, however, that our observations stem from noncanonical
363 cGAS pathways, such as PERK, that are independent of STING. Further study is needed to
364 decipher the context-dependent paradigm of cGAS activation and its downstream signaling
365 pathways in SSc-ILD and related conditions.

366 In terms of therapeutic potential, cGAS inhibition remains an active area of investigation
367 for clinical benefit. Currently available antagonists include the anti-malarial agents
368 hydroxychloroquine and quinacrine, which bind to the minor groove of the DNA-cGAS interface
369 to disrupt ligand-receptor interactions [29]. Suramin, a drug indicated for the treatment of river
370 blindness and African sleeping sickness, acts as a DNA mimic that competitively binds to cGAS
371 and inhibits 2,3,-cGAMP synthesis [30]. While repurposing these agents for SSc-ILD is a
372 consideration, the potential for non-specific, off-target effects limits their widespread use [31,
373 32]. Thus, the identification of compounds that directly inhibit cGAS has been actively pursued.
374 One promising compound was RU.521, which occupies the catalytic site of cGAS to inhibit
375 generation of 2,3,-cGAMP [31]. However, this effect was only seen in mouse studies, propelling
376 the development of G140, a human-specific small molecule inhibitor of cGAS with a mechanism
377 of action similar to RU.521 [23]. Moreover, relative to similar compounds, G140 demonstrated
378 superior efficacy inhibiting production of various lipopolysaccharide-induced cytokines in mouse
379 lung injury models [32]. Our study is the first to evaluate G140 in this inflammatory fibrotic
380 setting, and further work is needed for testing this agent in SSc-ILD human cohorts.

381 While novel and thought-provoking, our findings raise additional questions for future
382 research. Although we have identified fibroblasts as one site of activated cGAS function,
383 additional cell types are likely involved. Mechanistically, we have not determined if cGAS
384 activation mediates canonical versus non-canonical TGF β activation, nor its interactions with
385 mechanosensitive signaling, such as those involving Hippo [33], YAP [34], FAK [34], and Rho
386 associated kinase [35]. In terms of the cGAS ligand, we have not determined the contribution of

387 DNA derived from mitochondrial, nuclear, or even microbial sources. Moreover, we have yet to
388 determine the impact of canonical cGAS signaling components, such as the second messenger
389 protein 2,3,-cGAMP and STING. Lastly, we have not evaluated how cGAS inhibition compares
390 to immunosuppressive strategies [5] and anti-fibrotic agents [36] that are currently in use.
391 Despite these relatively minor limitations, in the first of its kind study, we found that cGAS is
392 expressed in SSc-ILD lung tissues and that its inhibition mitigates the development of
393 inflammatory fibrosis in cellular, tissue-based, and animal models. Further investigation may
394 yield the development of cGAS targeted therapies for SSc-ILD and related conditions.

395

396 **ACKNOWLEDGMENTS**

397 To all of our patients with scleroderma: the authors commend your bravery and resilience in
398 combatting this relentless disease. We hope and encourage you all to live your best lives.

399

400 **REFERENCES**

- 401 1. Denton, C.P. and D. Khanna, *Systemic sclerosis*. *Lancet*, 2017. **390**(10103): p.
402 1685-1699.
- 403 2. Herzog, E.L., et al., *Review: interstitial lung disease associated with systemic*
404 *sclerosis and idiopathic pulmonary fibrosis: how similar and distinct?* *Arthritis*
405 *Rheumatol*, 2014. **66**(8): p. 1967-78.
- 406 3. Steen, V.D. and T.A. Medsger, *Changes in causes of death in systemic sclerosis,*
407 *1972-2002*. *Ann Rheum Dis*, 2007. **66**(7): p. 940-4.
- 408 4. Rahaghi, F.F., et al., *Expert consensus on the management of systemic*
409 *sclerosis-associated interstitial lung disease*. *Respiratory Research*, 2023. **24**(1):
410 p. 6.
- 411 5. Raghu, G., et al., *Treatment of Systemic Sclerosis–associated Interstitial Lung*
412 *Disease: Evidence-based Recommendations. An Official American Thoracic*
413 *Society Clinical Practice Guideline*. *American Journal of Respiratory and Critical*
414 *Care Medicine*, 2023. **209**(2): p. 137-152.
- 415 6. Johnson, S.R., et al., *2023 American College of Rheumatology (ACR)/American*
416 *College of Chest Physicians (CHEST) Guideline for the Treatment of Interstitial*
417 *Lung Disease in People with Systemic Autoimmune Rheumatic Diseases*.
418 *Arthritis & Rheumatology*, 2024. **76**(8): p. 1182-1200.
- 419 7. Valenzi, E., et al., *Single-cell analysis reveals fibroblast heterogeneity and*
420 *myofibroblasts in systemic sclerosis-associated interstitial lung disease*. *Ann*
421 *Rheum Dis*, 2019. **78**(10): p. 1379-1387.
- 422 8. Reyfman, P.A., et al., *Single-Cell Transcriptomic Analysis of Human Lung*
423 *Provides Insights into the Pathobiology of Pulmonary Fibrosis*. *Am J Respir Crit*
424 *Care Med*, 2019. **199**(12): p. 1517-1536.
- 425 9. Gaydosik, A.M., et al., *Single-cell transcriptome analysis identifies skin-specific*
426 *T-cell responses in systemic sclerosis*. *Ann Rheum Dis*, 2021. **80**(11): p. 1453-
427 1460.
- 428 10. Ryu, C., et al., *Bioactive Plasma Mitochondrial DNA Is Associated With Disease*
429 *Progression in Scleroderma-Associated Interstitial Lung Disease*. *Arthritis &*
430 *Rheumatology*, 2020. **72**(11): p. 1905-1915.
- 431 11. Ryu, C., et al., *Extracellular Mitochondrial DNA Is Generated by Fibroblasts and*
432 *Predicts Death in Idiopathic Pulmonary Fibrosis*. *Am J Respir Crit Care Med*,
433 2017. **196**(12): p. 1571-1581.
- 434 12. Ryu, C., et al., *Bioactive Plasma Mitochondrial DNA Is Associated With Disease*
435 *Progression in Scleroderma-Associated Interstitial Lung Disease*. *Arthritis*
436 *Rheumatol*, 2020. **72**(11): p. 1905-1915.
- 437 13. Bueno, M., et al., *PINK1 attenuates mtDNA release in alveolar epithelial cells*
438 *and TLR9 mediated profibrotic responses*. *PLoS One*, 2019. **14**(6): p. e0218003.
- 439 14. Sun, L., et al., *Cyclic GMP-AMP synthase is a cytosolic DNA sensor that*
440 *activates the type I interferon pathway*. *Science (New York, N.Y.)*, 2013.
441 **339**(6121): p. 786-791.
- 442 15. Hopfner, K.P. and V. Hornung, *Molecular mechanisms and cellular functions of*
443 *cGAS-STING signalling*. *Nat Rev Mol Cell Biol*, 2020. **21**(9): p. 501-521.

- 444 16. Decout, A., et al., *The cGAS-STING pathway as a therapeutic target in*
445 *inflammatory diseases*. Nat Rev Immunol, 2021. **21**(9): p. 548-569.
- 446 17. Arwert, E.N., et al., *STING and IRF3 in stromal fibroblasts enable sensing of*
447 *genomic stress in cancer cells to undermine oncolytic viral therapy*. Nat Cell Biol,
448 2020. **22**(7): p. 758-766.
- 449 18. Sladitschek-Martens, H.L., et al., *YAP/TAZ activity in stromal cells prevents*
450 *ageing by controlling cGAS-STING*. Nature, 2022. **607**(7920): p. 790-798.
- 451 19. Schuliga, M., et al., *Self DNA perpetuates IPF lung fibroblast senescence in a*
452 *cGAS-dependent manner*. Clin Sci (Lond), 2020. **134**(7): p. 889-905.
- 453 20. Paul, S., et al., *Centromere defects, chromosome instability, and cGAS-STING*
454 *activation in systemic sclerosis*. Nat Commun, 2022. **13**(1): p. 7074.
- 455 21. Ishikawa, G., et al., *α 1 Adrenoreceptor antagonism mitigates extracellular*
456 *mitochondrial DNA accumulation in lung fibrosis models and in patients with*
457 *idiopathic pulmonary fibrosis*. American Journal of Physiology-Lung Cellular and
458 Molecular Physiology, 2023. **324**(5): p. L639-L651.
- 459 22. Zhou, Y., et al., *Chitinase 3-like 1 suppresses injury and promotes*
460 *fibroproliferative responses in Mammalian lung fibrosis*. Sci Transl Med, 2014.
461 **6**(240): p. 240ra76.
- 462 23. Lama, L., et al., *Development of human cGAS-specific small-molecule inhibitors*
463 *for repression of dsDNA-triggered interferon expression*. Nature
464 Communications, 2019. **10**(1): p. 2261.
- 465 24. Sun, H., et al., *Netrin-1 Regulates Fibrocyte Accumulation in the Decellularized*
466 *Fibrotic Sclerodermatous Lung Microenvironment and in Bleomycin-Induced*
467 *Pulmonary Fibrosis*. Arthritis Rheumatol, 2016. **68**(5): p. 1251-61.
- 468 25. Alsafadi, H.N., et al., *An ex vivo model to induce early fibrosis-like changes in*
469 *human precision-cut lung slices*. Am J Physiol Lung Cell Mol Physiol, 2017.
470 **312**(6): p. L896-L902.
- 471 26. Fang, F., et al., *Toll-like Receptor 9 Signaling Is Augmented in Systemic*
472 *Sclerosis and Elicits Transforming Growth Factor beta-Dependent Fibroblast*
473 *Activation*. Arthritis Rheumatol, 2016. **68**(8): p. 1989-2002.
- 474 27. Li, R., et al., *cGAS/STING signaling in the regulation of rheumatoid synovial*
475 *aggression*. Ann Transl Med, 2022. **10**(8): p. 431.
- 476 28. Yu, C.H., et al., *TDP-43 Triggers Mitochondrial DNA Release via mPTP to*
477 *Activate cGAS/STING in ALS*. Cell, 2020. **183**(3): p. 636-649.e18.
- 478 29. An, J., et al., *Cutting Edge: Antimalarial Drugs Inhibit IFN- β Production through*
479 *Blockade of Cyclic GMP-AMP Synthase–DNA Interaction*. The Journal of
480 Immunology, 2015. **194**(9): p. 4089-4093.
- 481 30. Wang, M., et al., *Suramin potently inhibits cGAMP synthase, cGAS, in THP1*
482 *cells to modulate IFN- β levels*. Future Medicinal Chemistry, 2018. **10**(11): p.
483 1301-1317.
- 484 31. Vincent, J., et al., *Small molecule inhibition of cGAS reduces interferon*
485 *expression in primary macrophages from autoimmune mice*. Nature
486 Communications, 2017. **8**(1): p. 750.
- 487 32. Tan, J., et al., *Synthesis and Pharmacological Evaluation of Tetrahydro- γ -*
488 *carboline Derivatives as Potent Anti-inflammatory Agents Targeting Cyclic GMP–*
489 *AMP Synthase*. Journal of Medicinal Chemistry, 2021. **64**(11): p. 7667-7690.

- 490 33. Deng, Q., et al., *Cross-Talk Between Mitochondrial Fusion and the Hippo*
491 *Pathway in Controlling Cell Proliferation During Drosophila Development.*
492 *Genetics*, 2016. **203**(4): p. 1777-88.
- 493 34. Nagaraj, R., et al., *Control of mitochondrial structure and function by the*
494 *Yorkie/YAP oncogenic pathway.* *Genes Dev*, 2012. **26**(18): p. 2027-37.
- 495 35. Wang, W., et al., *Mitochondrial fission triggered by hyperglycemia is mediated by*
496 *ROCK1 activation in podocytes and endothelial cells.* *Cell Metab*, 2012. **15**(2): p.
497 186-200.
- 498 36. Distler, O., et al., *Nintedanib for Systemic Sclerosis–Associated Interstitial Lung*
499 *Disease.* *New England Journal of Medicine*, 2019. **380**(26): p. 2518-2528.

500

501 **Table 1. Demographic and clinical characteristics of study participants.**

	Healthy controls	SSc without ILD	SSc-ILD
N	12	8	15
Age (mean ± SD)	53.04 ± 14.97	51.89 ± 10.67	60.10 ± 9.70
Gender (n, % female)	6 (50.0%)	8 (100%)	10 (66.7%)
Race			
White (n, %)	9 (75.0%)	6 (75%)	12 (80.0%)
Black (n, %)	3 (25.0%)	1 (12.5%)	2 (13.3%)
Other (n, %)	0 (0%)	1 (12.5%)	1 (6.7%)
Smoking			
Ever (n, %)	2 (16.7%)	3 (37.5%)	7 (44.7%)
Never (n, %)	10 (83.3%)	5 (62.5%)	8 (53.3%)
SSc Subtype			
Diffuse (n, %)	N/A	1 (12.5%)	5 (33.3%)
Limited (n, %)	N/A	7 (87.5%)	10 (66.7%)
Disease Duration (mean ± SD)	N/A	4.50 +/- 2.77	6.44 +/- 3.71
MRSS (median +/- IQR)	N/A	4.5 +/- 6.75	7.0 +/- 3.00
Scl-70 (n, %)	N/A	2 (25%)	7 (46.7%)
Centromere (n, %)	N/A	5 (62.5%)	3 (20.0%)
RNA Pol III (n, %)	N/A	0 (0%)	3 (20.0%)
None (n, %)	N/A	1 (12.5%)	2 (13.3%)
FVC% (mean ± SD)	N/A	90.00 ± 18.98	80.22 ± 19.19
DLCO% (mean ± SD)	N/A	91.14 ± 22.83	64.89 ± 24.80

502

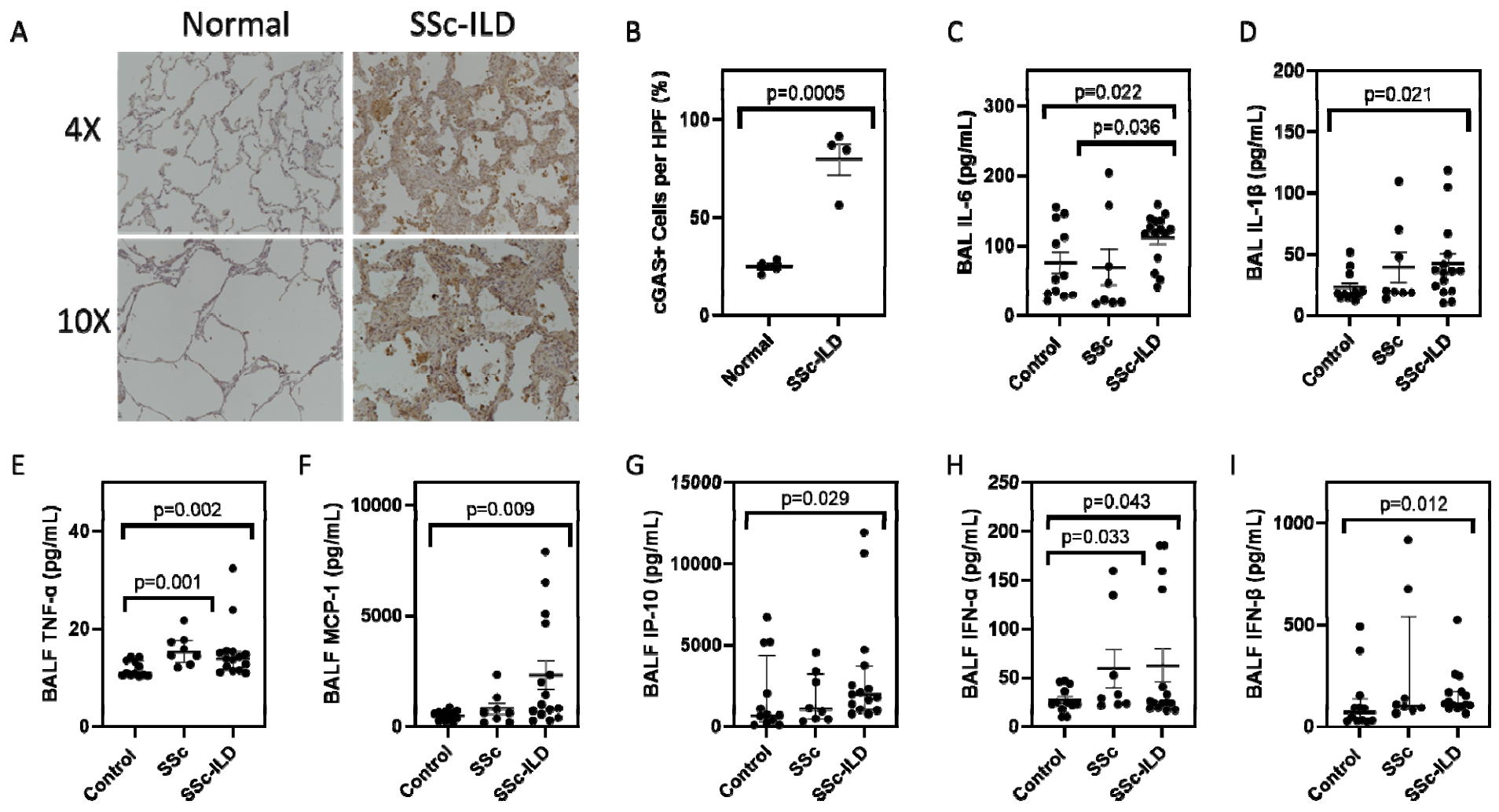


Figure 1. SSc-ILD lungs show enhanced expression of cGAS and its associated inflammatory mediators. (A) IHC for cGAS showed enhanced detection in the SSc-ILD lung (right) as compared to the normal lung (left). **(B)** A higher percentage of cGAS positive cells (per high-powered field) was observed in the SSc-ILD lung. BAL fluid samples collected from healthy donors and SSc patients showed that relative to healthy participants, SSc-ILD patients exhibited increased concentrations of **(C)** IL-6, **(D)** IL-1 β , **(E)** TNF- α , **(F)** MCP-1, **(G)** IP-10, **(H)** IFN- α , and **(I)** IFN- β .

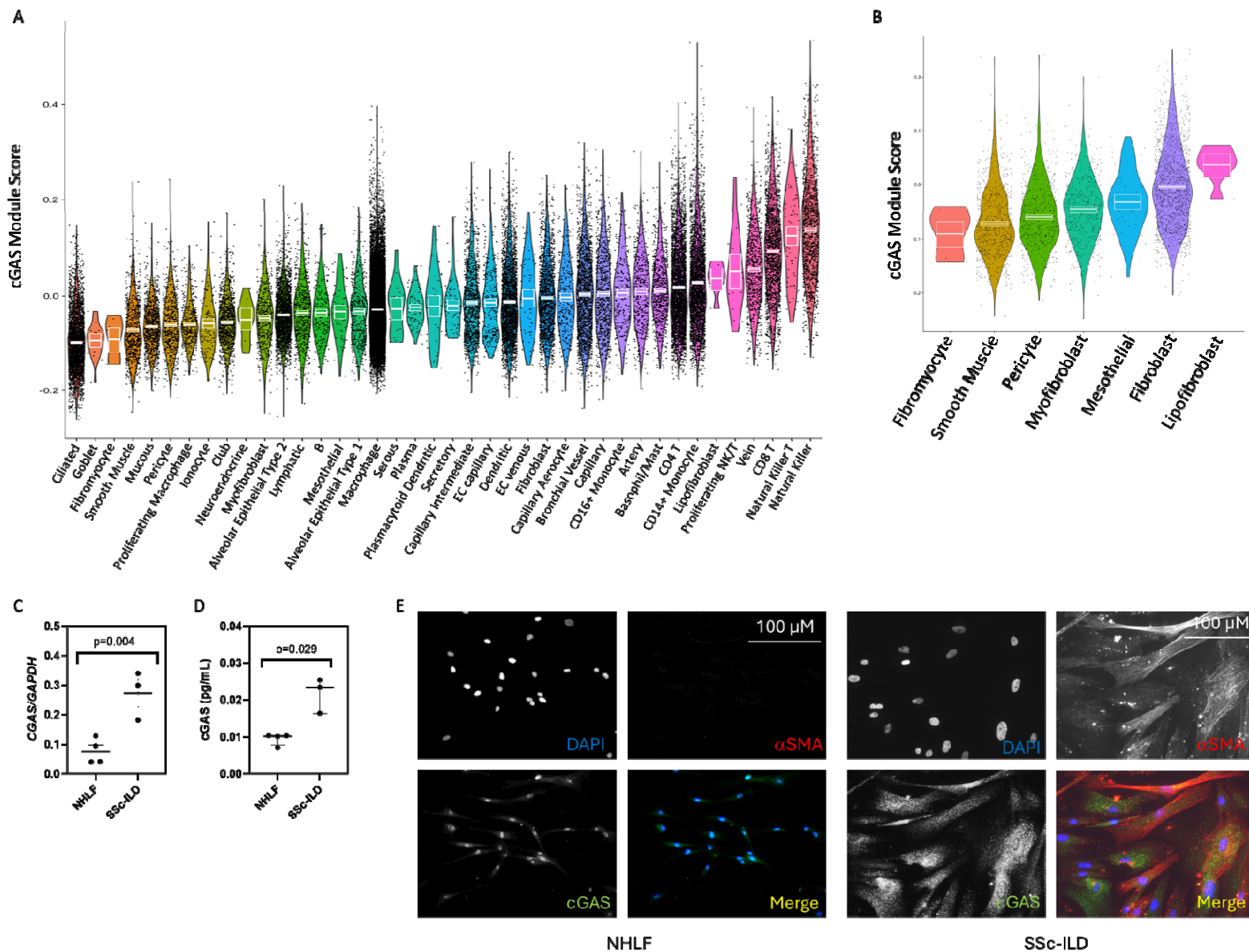


Figure 2. SSc-ILD lung fibroblasts are enriched for cGAS expression. (A) Violin plot of single cell RNA sequencing analysis (derived from GEO dataset GSE128169) from the lungs of patients with SSc-ILD demonstrating median expression of cGAS-related genes across multiple cell populations, which was highest among immune and endothelial cells. (B) Among stromal cells, fibroblasts (purple) demonstrated enhanced expression of these genes. (C) qRT-PCR and (D) ELISA measurements of NHLFs and SSc-ILD fibroblasts showed increased transcription and protein expression of cGAS in SSc-ILD fibroblasts. (E) IF evaluation of NHLFs (left) and SSc-ILD fibroblasts (right) showed the increased presence of α SMA and cytoplasmic aggregation of cGAS in SSc-ILD fibroblasts (versus the nuclear localization of cGAS in NHLFs). Scale bar = 100 microns.

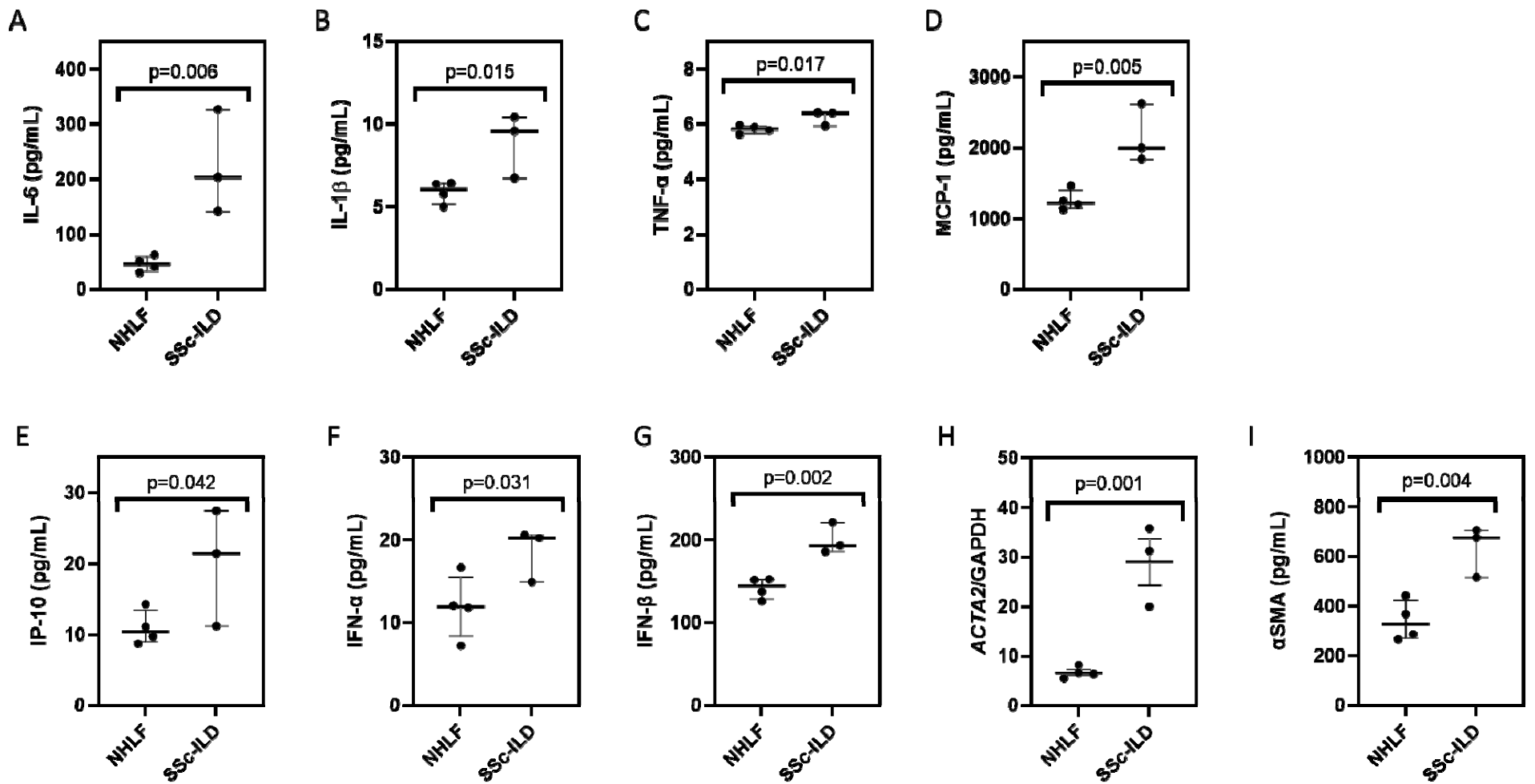


Figure 3. SSc-ILD fibroblasts express high concentrations of cGAS associated soluble mediators and α SMA. As compared to NHLFs, SSc-ILD fibroblasts expressed high protein levels of (A) IL-6, (B) IL-1 β , (C) TNF- α , (D) MCP-1, (E) IP-10, (F) IFN- α , and (G) IFN- β . Relative to normal cells, SSc-ILD fibroblasts expressed increased α SMA (H) transcripts via RT-qPCR and (I) protein via ELISA.

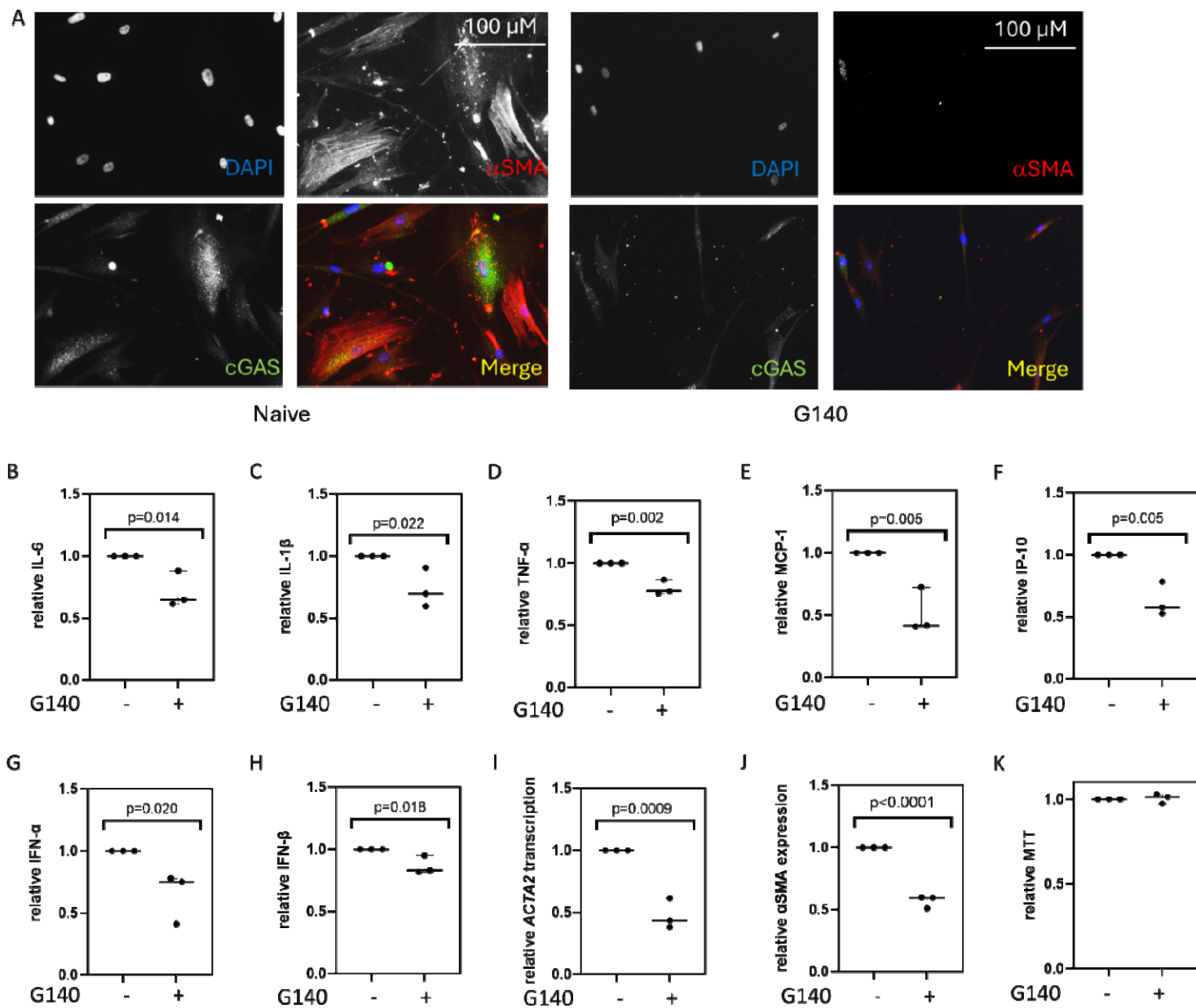


Figure 4. Small molecule cGAS inhibition mitigates inflammatory fibrotic responses in SSc-ILD fibroblasts. (A) IF staining of naïve (left) and G140 treated (right) SSc-ILD fibroblasts showed reduced detection of both cytoplasmic cGAS aggregates and α SMA in treated cells. Scale bar = 100 microns. These G140-treated cells displayed decreased expression of (B) IL-6, (C) IL-1 β , (D) TNF- α , (E) MCP-1, (F) IP-10, (G) IFN- α , and (H) IFN- β . Treated cells also displayed a reduction in the (I) transcription and (J) protein expression of α SMA. (K) An MTT assay showed that G140 did not influence the viability of these fibroblasts. Data was normalized to the untreated condition.

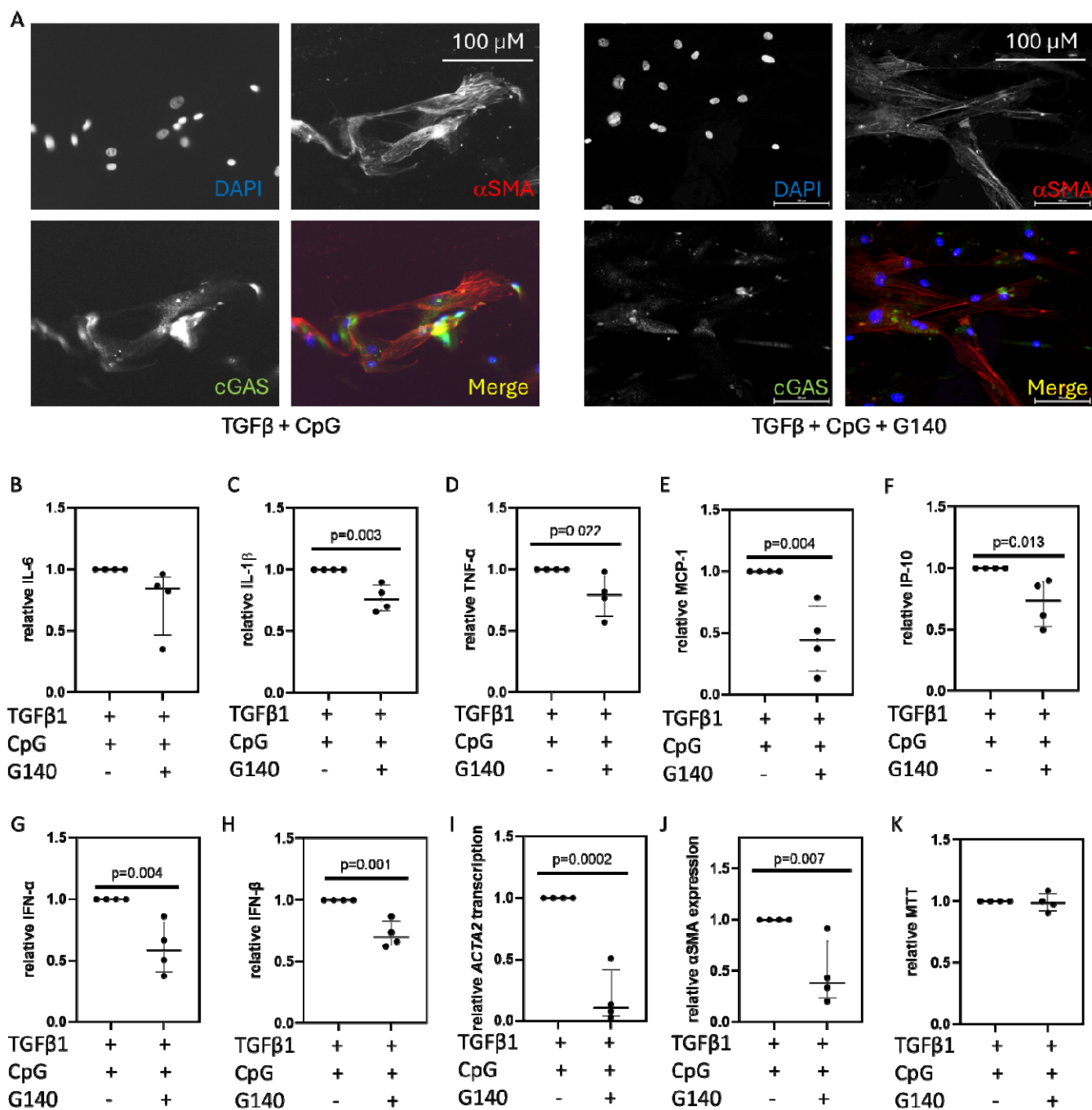


Figure 5. A small molecule cGAS inhibitor suppresses inflammatory fibroblast activation induced by TGFβ1 and CpG co-stimulation. (A) IF of NHLFs co-stimulated with TGFβ1 and CpG in the absence (left) or presence (right) of G140 showed that treatment diminished the presence of cGAS aggregates in the cytoplasm. Scale bar = 100 microns. Although treatment with G140 did not change levels of **(B)** IL-6, it attenuated expression of **(C)** IL-1β, **(D)** TNF-α, **(E)** MCP-1, **(F)** IP-10, **(G)** IFN-α, and **(H)** IFN-β, as well as **(I)** mRNA transcription and **(J)** protein expression of αSMA. **(K)** An MTT assay showed that these findings were unrelated to changes in cell viability. Data were normalized to the TGFβ1 + CpG condition.

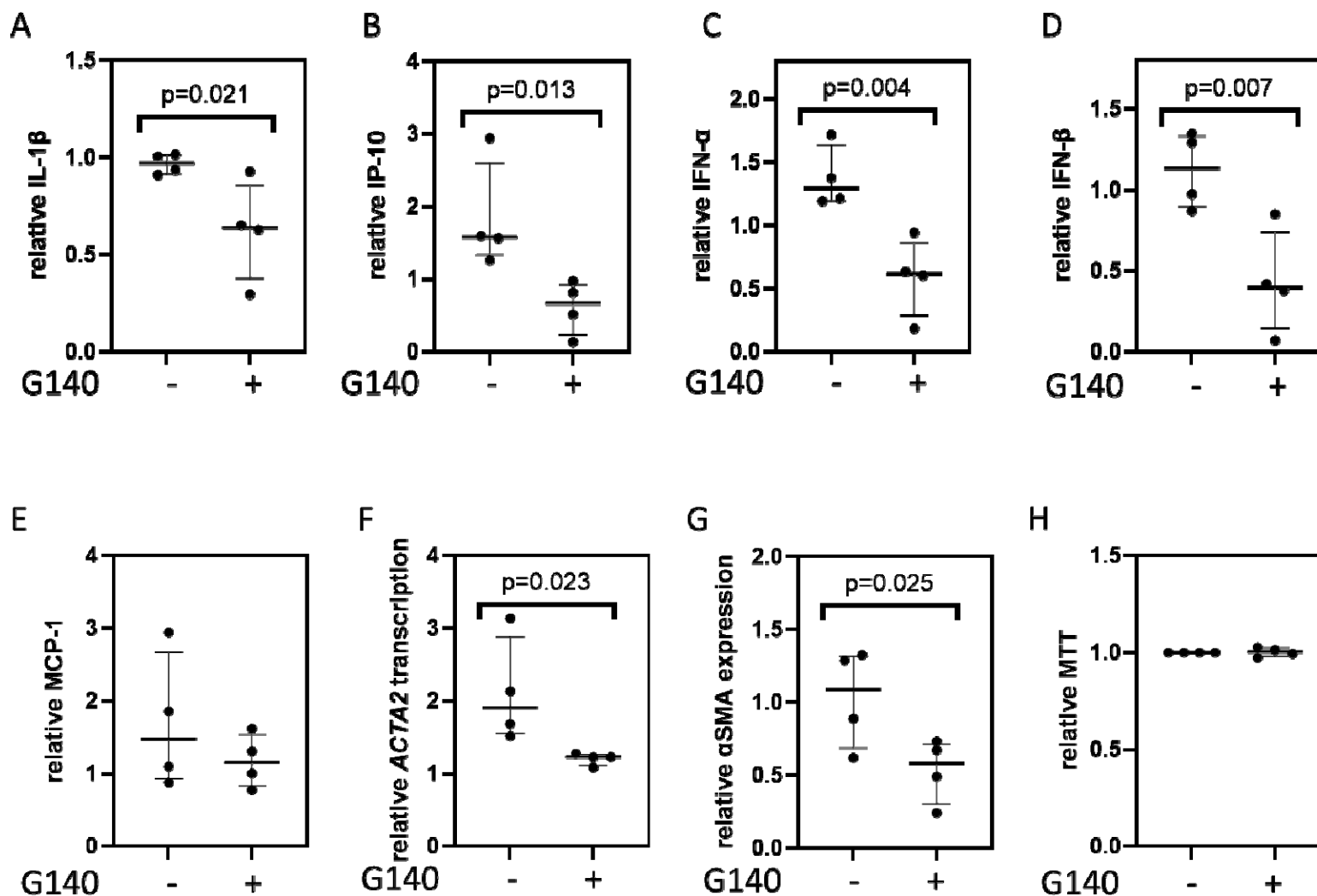


Figure 6. A small molecule cGAS inhibitor mitigates stiffness-induced fibroblast activation. NHLFs were cultured on tunable hydrogels that approximate the stiffness of the normal (1kPA) and fibrotic (25 kPA) lung. As compared to NHLFs cultured in the untreated 25 kPA condition, those grown on 25 kPA hydrogels treated with G140 exhibited decreased levels of **(A)** IL-1 β , **(B)** IP-10, **(C)** IFN- α , and **(D)** IFN- β ; expression of **(G)** MCP-1 remained unchanged. This inhibitor also led to a reduction in the **(F)** transcription and **(G)** expression of α SMA. **(H)** An MTT assay showed that these findings were unrelated to changes in cell viability. Data was normalized to their respective untreated or treated 1 kPA condition.

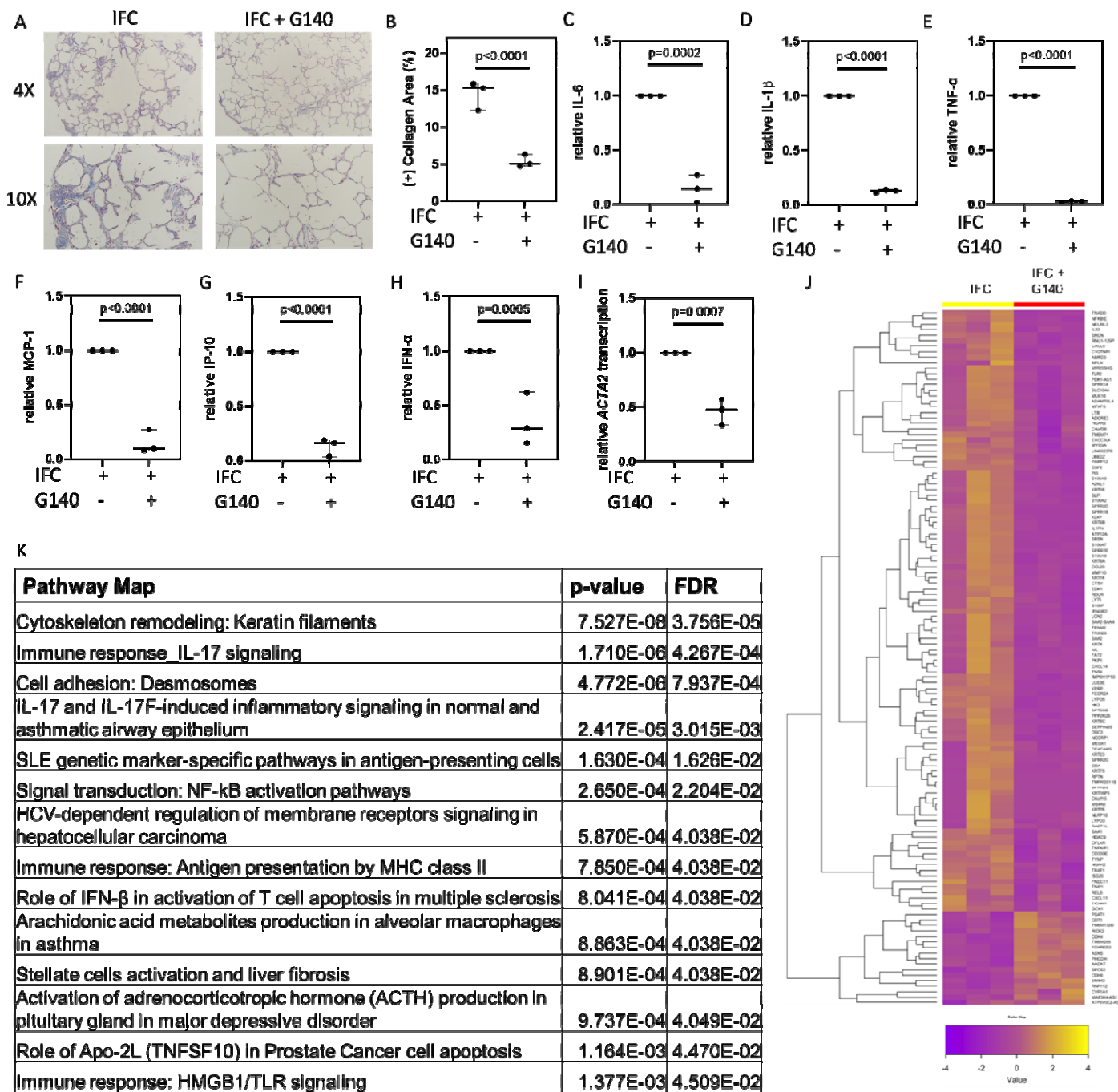


Figure 7. A small molecule cGAS inhibitor abrogates inflammatory fibrotic responses in human precision cut lung slices. (A) Representative images of Masson's Trichrome staining of human PCLS sections from those subjected to an inflammatory fibrotic cocktail (IFC) in the absence (left) or presence (right) of G140. (B) Collagen quantification via ImageJ software revealed a reduction in collagen content following treatment with G140. Treatment with this inhibitor mitigated expression of (C) IL-6, (D) IL-1 β , (E) TNF- α , (F) MCP-1, (G) IP-10, and (H) IFN- α , and transcription of (I) ACTA2. Data were normalized to the IFC condition. (J) Heatmap of bulk RNA sequencing between IFC cultured PCLS in the absence or presence of G140 revealed 126 differentially expressed genes (DEGs). (K) Unbiased pathway enrichment analysis.

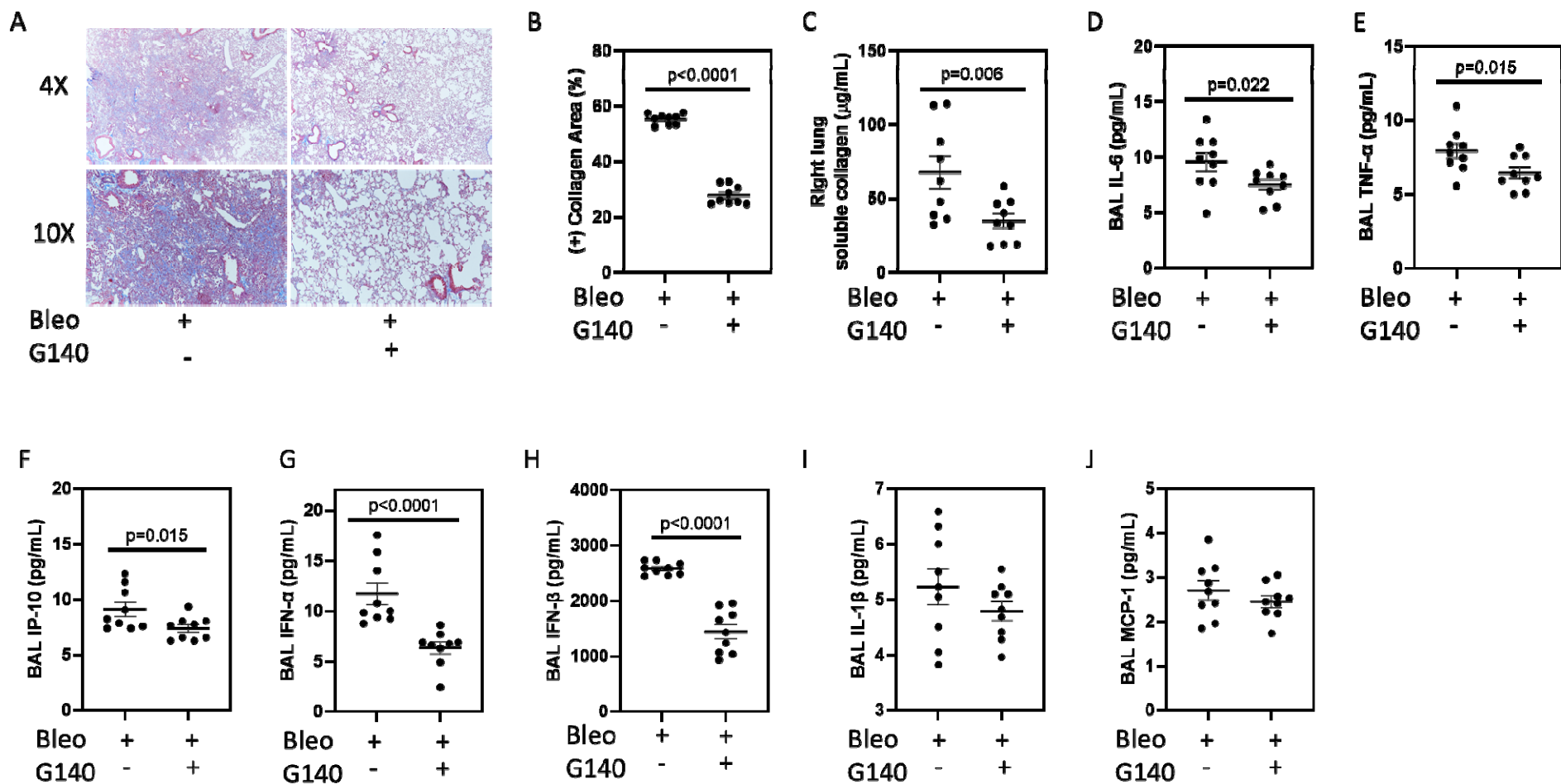


Figure 8. A small molecule cGAS inhibitor ameliorates bleomycin induced pulmonary fibrosis. (A) Representative images of Masson's Trichrome staining of lung sections from bleomycin challenged mice in the absence (left) or presence (right) of G140. Collagen quantification via (B) ImageJ software and (C) Sircol assay revealed a reduction in collagen content following treatment with G140. Bleomycin exposed mice treated with G140 displayed reduced BAL concentrations of (D) IL-6, (E) TNF- α , (F) IP-10, (G) IFN- α , and (H) IFN- β , while levels of (I) IL-1 β and (J) MCP-1 remained unchanged.